JOURNAL OF AIRCRAFT
Vol. 45, No. 6, November–December 2008

Airplane Landing Performance on Contaminated Runways in Adverse Conditions

Nihad E. Daidzic* and Juna Shrestha†
Minnesota State University, Mankato, Minnesota 56001

DOI: 10.2514/1.38056

A realistic analysis of operational landing and stopping performance of large-transport-category airplanes on contaminated runways in adverse conditions is presented. A new mathematical model of landing flare is introduced. Heaviside step functions were employed to model the time-delayed deployment of ground spoilers, brakes, and thrust reversers and to account for variations in pilot techniques. A simulation model, based on submodels for each landing phase, consists of several distinct systems of simultaneous nonlinear coupled ordinary differential equations, semi-empirical models, and many accompanying algebraic relationships for aerodynamic coefficients and other parameters. The full nonlinear differential model was solved numerically using the simple Heun's predictor-corrector method. Different landing scenarios were simulated to obtain realistic stopping distances as well as the time histories of deceleration and speed. The model accounts for many contaminated runway scenarios, hydroplaning, the effect of wind, the speed-dependent rolling-friction coefficient, and other important parameters. We have presented landing scenarios using average pilot techniques on ice-covered runways for which the Federal Aviation Administration wet-runway safety factor is not sufficient for a safe landing. This mathematical model and the simulation program can be used as an operational landing distance calculator. A sensitivity analysis was performed to estimate the significance of various parameters with the absolute maximum landing distance uncertainty estimated to be 100 ft.

Nomenclature

AR	=	aspect ratio,
b	=	wing span, m or ft
C_D	=	drag coefficient
C_L	=	lift coefficient
e	=	Oswald's coefficient
g	=	gravitational acceleration, m^2/s or ft^2/s
h	=	height, m or ft
n	=	load coefficient
S	=	wing reference area, m^2 or ft^2
s	=	landing distance, m or ft
T	=	thrust, N or lbf
v	=	airspeed; m/s, ft/s, or kt
v_{so}	=	stalling airspeed in landing configuration; m/s, ft/s, or kt
W	=	weight, kg or lbm

Greek

α	=	angle of attack, deg
γ	=	glide path angle (gradient); %, deg, or rad
δ	=	thrust inclination angle, rad or deg
ζ	=	wind correction factor
θ	=	pitch angle, rad or deg
Φ	=	runway inclination (gradient); %, deg, or rad
φ	=	angle between gear touchdown trajectory and runway, rad or deg
ψ	=	pitch rate, rad/s or deg /s

Subscripts

A	=	air
APP	=	approach
FL	=	flare
FLGS	=	flare and groundspeed
FLH	=	flare height
G	=	ground (ground effect)
GR	=	ground roll
GS	=	ground speed
LD	=	landing
NGTD	=	nose gear touchdown
NGUP	=	nose gear up
R	=	rolling with brakes off
rb	=	rolling with brakes on
REF	=	reference
REV	=	reverse (thrust)
TAS	=	true airspeed
TCH	=	threshold
TD	=	touchdown
W	=	wind

I. Introduction

THE final approach and landing constitute only about 2% of the average total flight time, yet almost 50% of all aviation accidents and incidents occur during this phase [1,2]. The reasons for this are many, but the most significant ones are that both the pilot workload and pilot fatigue are at the highest level, coinciding with the narrowest margin of safety. Operating close to the ground in a fast moving aircraft is the most hazardous part of the flight and requires a maximum of the pilot's skills [1]. The majority of landing accidents, though usually not fatal, are either overrun or runway excursion accidents. According to Blake and Elliott [1], there is one landing overrun per 3.6 million flights. In 1990, that would have been one landing overrun every 3 months [1]. The accident statistics have confirmed those figures. Lowery [3] and Gugeler [4] reported that about 42% of all general aviation (GA) accidents occur during the final approach-and-landing phase. Lowery [3] also stated that most of the landing incidents and accidents are indeed overrun accidents in

Received 14 April 2008; accepted for publication 14 June 2008.

*Associate Professor of Aviation and an Adjunct Associate Professor of Mechanical Engineering, Aviation Department, Armstrong Hall 324E; Nihad.Daidzic@mnsu.edu. Member AIAA.

†Undergraduate Student, Department of Mathematics and Statistics, 273 Wissink Hall.

which an airplane skidded off the end of the runway. Citing Boeing's original sources, Bibel [5] claims that landing mishaps cause 45% of all accidents in commercial air transportation. Takeoffs are a distant second with the 12% of total aviation accidents. Typically, landing (or takeoff) consumes only 1% of the total flight time in commercial air transportation. About 2% of the total fatalities occur during the landing phase. Bibel [5] has devoted a whole chapter to the human tolerance of g loads and crash forces, which is an important part of understanding survivability during landing (and other) accidents.

Usually, in landing accidents, the runway was too short for the existing conditions, which were wet, slushy, snow covered, etc. Some of the contributing factors are mechanical systems failures, such as brake, antiskid, lift-dump spoiler deployment, or reverse-thrust (cannot be credited toward landing stop) malfunctions. For example, on 4 November 1993 at the old Hong Kong Kai-Tak airport, China Airlines Boeing 747 veered off the wet surface with significant crosswind and the airplane skidded off the runway, ending up in the harbor, luckily with no fatalities. However, many passengers and crew members died in an attempted go-around after the long touchdown in an American Airlines B727-100 landing at St. Thomas airport (Virgin Islands) in April 1976 [6]. The Boeing airliner touched down 3000 ft from the threshold of the 4650-ft-long runway and, after abandoning initial braking, unsuccessfully attempted the go-around. Go-arounds after the touchdown can be very hazardous in large-transport-category jet airplanes. Spool time to full thrust after the throttles have been pulled to idle can take 3–4 s in a new generation turbofans vs 7–8 s in the older low-bypass ratio JT8Ds. Also, reconfiguring flaps for takeoff/go-around and stowing spoilers and/or thrust reversers might take too long. Often, landing overruns are caused due to the unstabilized approach.

Undershoot landing accidents are less frequent and are mostly the result of windshear and strong wind gradient on the short final approach. They often are fatal, however. It is clear that the operations on contaminated runways and adverse weather conditions are the most hazardous landing operations [7,8]. Stephens [8] investigated a National Transportation Safety Board (NTSB) database of landing veer offs and overruns on contaminated runways in the period from 1962 to 1973 and made several recommendations, some of which were later adopted by the regulatory agencies. Recently, Marchi [7] reported on the status of the operational rolling-friction measurements and the difficulties and the progress the U.S. airports and the Federal Aviation Administration (FAA) are facing. McKinney [9] reported on the progress achieved so far in improving approach-and-landing safety. He also highlighted various recommendations for the reduction and elimination of approach-and-landing accidents that the Flight Safety Foundation (FSF) Approach-and-Landing Accident Reduction (ALAR) Force has implemented so far. Some of the "new" recommendations mirror the old well-known operational techniques but, despite all the efforts, the same errors and landing accidents/incidents still occur. A good description of various runway contaminants, associated hazards, and operational difficulties facing pilots and operators is given in [3,10–13]. In addition, Schiff [2], Davis [12], Denton [14], and Webb and Walker [15] describe some pilot techniques and recommendations for landings in adverse and contaminated runway conditions.

The probability of a landing mishap is the highest of all possible accidents in a typical commercial flight. However, presumably due to the relatively low number of fatalities or serious injuries, landing models and predictions have not attracted the attention that they most certainly deserve. In many engineering aircraft performance textbooks, mostly limited treatment is given to the landing process. Often very unrealistic and simplistic assumptions are employed. On the other hand, the pilot community uses many rules of thumb, often derived from experience, which usually cannot be just linearly superimposed to arrive at the corrected (factored) landing distances.

All of the earlier models commented and critiqued upon here were based on the classical Newton's law of motion for flat nonrotating earth. Thrust, drag, and rolling-friction forces were considered in more or less detail. Many authors did not consider the effect of runway gradient and/or the wind. In many previous studies, the air distance was simply a straight path to touchdown or a straight path descent followed by the semicircular flare trajectory resulting in a tangential touchdown with zero sink.

The first study of the landing or flare process that we cite was by White [16]. The author proposed a landing flare model that, in his own words, was not confirmed in all details. White correctly identified the effects of the thrust and the aerodynamic efficiency in the landing flare, but he also assumed an unrealistic float and deceleration of an airplane in the ground effect before touchdown. Pinsker's [17] work on the landing flare really stands out among all other works on this subject, as it is both in-depth and detailed. Pinsker identified many of the important effects during the landing flare, including the short-lived adverse elevator effect. He also discussed the benefits of the direct lift control (DLC) in landings, as well as the stability and control response augmentation. However, Pinsker, like many other authors, assumed tangential touchdown with zero vertical speed. Pinsker used the Laplace transform to solve the linearized differential equations of motion. Seckel [18] also derived a linearized model of the landing flare, in conjunction with the flight test involving a variable-stability GA aircraft. The author arrived at many useful conclusions about the landing maneuver. However, his analysis, like those already mentioned, only included landing flare and neither the approach phase nor the ground braking roll were considered.

Asselin [19], Mair and Birdsall [20], and Vinh [21] gave a simplified analysis of the landing maneuver. Many important forces and effects were included; however, the same assumption of the tangential touchdown was assumed. Some other unrealistic assumptions were employed as well. Vinh's analysis also includes several analytical solutions. Many authors performed a linearization of the nonlinear equations, and analytical solutions were derived for certain, rather severe, assumptions. However, Mair and Birdsall used several very useful semi-empirical relations, which make their approach to the subject somewhat more realistic. They also discussed the use of DLC, like Pinsker. Roskam and Lan [22] and Philips [23] delivered fairly in-depth analyses of the landing process. Analytical and numerical solutions were discussed. Roskam and Lan suggested using Simpson's numerical integration to solve the nonlinear ordinary differential equations (ODEs). Unfortunately, the same assumptions as mentioned earlier were adopted.

Croll and Martin [24] published a notable work on estimating landing distances and friction braking efficiency on winter-contaminated runway surfaces in Canada. However, they focused their research exclusively on the ground run and the ground stopping distance with ice and/or snow contamination. Their inclusion of the air distances in the total landing distances is very basic. A special strength of their work is the experimental tests using the Falcon 20 jet. However, the authors were not able to achieve a consistent trend in the braking coefficient dependence on the plane's ground speed. On the other hand, Yager [25] was successful in establishing variations and trends in the braking coefficient with aircraft speed for dry and contaminated runways using NASA's B737-100 aircraft. Visser [26] presented a problem of an approach-to-landing maneuver using thrust-vectoring aircraft. This method only applies to high-performance military aircraft. Visser used numerical integration and optimization to obtain the approach-and-landing trajectories of the high angle of attack (AOA) thrust-vectoring aircraft (extremely short takeoff and landing, or ESTOL). Visser did not consider the landing ground roll as it would then be a conventional stopping problem once the aircraft is on the runway. His analysis is not directly applicable to the landing problem of a transport-category aircraft certified under Title 14, Code of Federal Regulations (CFR) Part 25, but we found his approach very useful in many respects.

II. Landing Maneuvers

A. National Transportation Safety Board Reports on Landing Accidents

It is impossible to mention here more than just a few typical runway overrun accidents from the vast accident and incident databases. However, it is worth saying that, even today, runway veer offs, overruns, and excursions occur with persistent regularity. As a

matter of fact, every month, somewhere in the world, there is, on average, one serious landing or rejected-takeoff runway overrun accident involving a transport-category airplane. To support some of the statements mentioned here, and the rationale and the motivation for our research, we are presenting verbatim some excerpts from two NTSB final reports on landing accidents. The first, NTSB report DCA99MA060 [27], states

> On June 1, 1999, at 2350:44 central daylight time, American Airlines flight 1420, a McDonnell Douglas DC-9-82 (MD-82), N215AA, crashed after it overran the end of runway 4R during landing at Little Rock National Airport in Little Rock, Arkansas. Flight 1420 departed from Dallas/Fort Worth International Airport, Texas, about 2240 with 2 flight crewmembers, 4 flight attendants, and 139 passengers aboard and touched down in Little Rock at 2350:20. After departing the end of the runway, the airplane struck several tubes extending outward from the left edge of the instrument landing system (ILS) localizer array, located 411 feet beyond the end of the runway; passed through a chain link security fence and over a rock embankment to a flood plain, located approximately 15 feet below the runway elevation; and collided with the structure supporting the runway 22L approach lighting system. The captain and 10 passengers were killed; the first officer, the flight attendants, and 105 passengers received serious or minor injuries; and 24 passengers were not injured. The airplane was destroyed by impact forces and a post crash fire. Flight 1420 was operating under the provisions of Title 14, CFR Part 121 on an instrument flight rules (IFR) flight plan.

The NTSB determined the probable cause(s) of this accident as follows

> The flight crew's failure to discontinue the approach when severe thunderstorms and their associated hazards to flight operations had moved into the airport area and the crew's failure to ensure that the spoilers had extended after touchdown. Contributing to the accident were the flight crew's (1) impaired performance resulting from fatigue and the situational stress associated with the intent to land under the circumstances, (2) continuation of the approach to a landing when the company's maximum crosswind component was exceeded, and (3) use of reverse-thrust greater than 1.3 engine pressure ratio after landing.

The following overrun accident happened to a Gemini Air Cargo, Inc., MD-11F [28]. The NTSB report NYC03IA117 states

> The cargo airplane was on approach to land at night, on runway 4R; an 8,400-foot-long, asphalt runway. The flight crew received the current automated terminal information service weather, which included winds from 240 degrees at 4 knots. The captain was the flying pilot. He stated that he utilized the autopilot to 500 feet, before clicking it off, and stayed on the glide slope. The airplane's landing weight was about 470,000 pounds, and it was configured for a normal approach, which included autobrakes set to minimum and 35 degrees of flaps. The captain reported that the airplane touched down between 1,500 and 1,800 feet beyond the approach end of the runway, at airspeed of about 158 knots. The captain applied reverse-thrust and everything seemed normal until he observed the alternating red and white runway lights, which seemed to be coming up fast. The captain stated that with about 3,000 feet of runway remaining, at a speed of 110 knots, he began to apply manual braking. The first officer stated he could feel the brakes grab, and the airplane's nose pitched down. The airplane departed the end of the runway and entered an Engineered Materials Arresting System (EMAS). The airplane's nose-gear came to rest approximately 238 feet beyond the end of the runway, 115 feet into the EMAS. Both flight crew members reported normal cockpit indications before, during, and after the incident. Post incident examination of the airplane, which included a brake inspection and an operational check of the autobrake system, did not reveal any faults or abnormalities. A recorded radar and performance study indicated that the airplane crossed the runway threshold at an altitude of about 60 to 120 feet above the ground. The main landing gear touched down approximately 2,800 to 3,000 feet from the beginning of runway 4R, and the nose-gear touched down at about 4,300 feet. The automatic braking system initiated approximately three seconds after nose wheel touchdown. The pilot initiated manual braking with about 1,400 feet of runway remaining. According to the operator's performance data for the airplane, the maximum landing weight allowed to utilized runway 4R for the incident landing configuration was 491,500 pounds in a zero-wind condition, and 452,800 pounds, with a 5 kn tailwind.

The NTSB determined the probable cause(s) of this incident as follows: *The Captain's misjudgment of speed/distance which resulted in his failure to obtain the proper touch point resulting in an overrun. Factors in this accident were the tail wind, and night light conditions.*

Also very illustrative and typical is the overrun landing accident of the Royal Air Maroc's Boeing 747-200 CN-RME that landed on an 8000 ft wet and slippery runway at Dorval/Montreal International Airport, Quebec, Canada [29]. In all three cases mentioned, an inadequate pilot technique and poor judgment contributed to the accident. In the second accident involving the cargo MD-11F, the airplane crossed the threshold at twice the altitude required, which resulted in the distant touchdown point. Subsequent improper braking action resulted in an overrun, although the runway was not even reported to be contaminated.

Especially troubling is a recent Southwest (SW) Boeing 737-700 landing overrun accident on the partly snow-covered and relatively short runway 31C at Chicago Midway (KMDW) Airport [30–32]. Johnsen [31] reports that the runway friction equipment reported braking action as "good" 30 min before and 10 min after the SW Boeing 737-700 overrun at KMDW.

B. Landing Phases

The landing maneuver consists of several distinct phases. One can roughly divide the landing maneuver into separate air and ground runs. In Fig. 1, the different landing phases are illustrated. Ideally, the landing gear threshold crossing heights (TCH) are between 35 and 50 ft [1]. After crossing the threshold, the airplane continues in a steady and stabilized descent to a "flare" height at which the flare (landing transition) maneuver is initiated. This consists of the pilot slightly pulling back on the control column (or side stick in an Airbus) and continuously increasing airplane's pitch and AOA, while simultaneously smoothly closing the throttles to idle. A great deal of latitude is possible here. The airplane will track a curved path due to the small upward vertical acceleration, reducing the rate of descent (ROD) to an acceptable 120 fpm (feet per minute) or less, while simultaneously touching down on the main gears at the runway centerline with no side drift and avoiding bounce, float, or ballooning. Normally, a main gear touchdown will occur within the runway touchdown zone as required by regulations [e.g., the International Civil Aviation Organization (ICAO); Federal Aviation Regulations (FAR) 25, 121, and 135; and the Joint Aviation Requirement on Commercial Air Transportation (JAR-OPS)]. This technique of simultaneously pitching up and continuously retarding the throttles throughout flare is called the *decelerate technique*, according to Seckel [18]. In reality, no significant deceleration

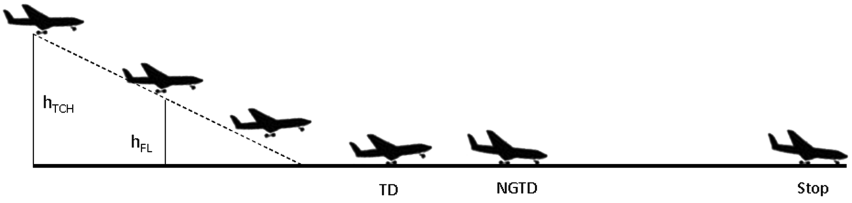

Fig. 1 Schematic drawing of the landing maneuver with all important segments (not to scale).

occurs because the time is short, the airplane is descending, and the ground effect reduction of induced drag will offset, in large part, the thrust retardation.

Slowing down while floating in a ground effect and preventing an airplane to touchdown (holding it off) is not a safe landing technique for large-transport-category airplanes [1–3,10–15]. After the main landing gears touch down, the nose gear will be lowered smoothly within the next few seconds. Now, after all the tires are firmly on the ground (and rotating), it is imperative to stop the airplane on the runway remaining. Relatively long runways give the operator more freedom to reduce brake and tire wear and tear by judiciously using thrust reversers. However, friction braking is still the most important operational deceleration technique. The friction braking depends strongly on the pilot technique, braking system (automatic braking system, antiskid), surface contamination, brake-torque limit, tire quality, normal reaction force, ground speed, etc.

To increase the normal reaction force and thereby increase the friction force between the tires and the runway surface, it is important to put as much airplane "weight" on the wheels as soon as possible. Even though the airplane is on the runway at a zero pitch angle, it will still produce a significant amount of lift. This is due to an increased incident angle from the deployed high-lift devices. Therefore, the deployment of the ground and flight spoilers after touchdown (lift-dump system) is an important tool for reducing the wing's coefficient of lift and thereby putting more weight on the tires. The aerodynamic drag is increased too, but that is not so significant.

Thrust reversing is another important stopping tool. Especially in the case of slippery runways, the thrust reversing system accomplishes most of the speed retardation effort. Aerodynamic braking, tail hooks, or ESTOL thrust-vectoring methods [26] are not acceptable techniques for landing civilian large-transport-category airplanes. Runway elevation plays a limited role in landing rollout. According to JAR-OPS aviation regulations, slopes of less than 2% need not be accounted for in landing distance calculations [13].

In general, the most important factors that affect the total landing distance are wind, airspeed, glide path angle, threshold crossing height, aircraft weight, airplane aerodynamics (e.g., high or low aspect ratio), air density (density altitude), pilot technique, and ground effect. Of all these, the pilot technique represents the largest uncertainty, as large variations in pilot performance and techniques exist. The purpose of airline standard operating procedures (SOPs) is to reduce the deviation and standardize pilot performance [3,9,12,15].

The FAA requires (CFR Secs. 25.175, 121.195, 121.197, etc.) that the dry-runway airplane (actual) demonstrated landing distance (DLD) is no longer than 60% of the available runway:

$$\text{DLDR} = (\text{DLD}/0.6) \approx 1.67 \times \text{DLD} \leq \text{LDA}$$

where LDA is the available landing distance that may or may not include the stopway and DLDR is the required dry landing distance. The DLDR can be equal to, or shorter than, the LDA, but never longer (DLDR $\leq$ LDA). In the case of a contaminated runway, the FAA mandates that 15% be added to the DLDR (U.S. Department of Transportation, FAA, Title 14, CFR 121 and 135) resulting in a "wet-runway" correction (WLDR $\leq$ LDA):

$$\text{WLDR} = 1.15 \times \text{DLDR} \approx 1.92 \times \text{DLD}$$

However, the FAA-mandated wet-runway safety factor does not differentiate between the various types of contamination, some of which are quite serious [1–3,10–15]. Inadequate pilot techniques or equipment malfunction can easily multiply the normal landing distances. In most cases, the regulations provide a safe margin for landing operations, but the overrun accident statistics show that there are cases in which even this mandatory safety factor is not sufficient for safe operations [2,3,13,15]. Therefore, pilots cannot be always blamed for the landing accidents.

Several attempts by industry experts and groups have been initiated in the past to eliminate or at least reduce overrun accidents. A study of pilot techniques and operations was conducted recently by the FSF ALAR international task force [9]. Many conclusions and recommendations regarding SOP have been suggested and it is hoped that the ALAR initiative will help considerably reduce the number of landing accidents worldwide.

The main objective of this study is to develop a reliable, realistic, and operationally useful landing calculator and to highlight relevant physical phenomena and their interactions with the landing process. We are also introducing some new and more accurate submodels and concepts of landing phases, and we have designed a program written in MATLAB® that has many features previously unavailable, to the best of our knowledge, in any similar study. Some of the simulated features include realistic pilot performance, realistic airplane dynamics, runway conditions, atmospheric and weather conditions, and real-life operations. We also attempted to simulate the realistic operations of the brakes, lift-dump system, flaps, thrust reversers, pilot reaction times, and other factors. An extensive database consisting of runway rolling-friction coefficients data based on experimental results [24,25,33–35] and hydroplaning dynamics on wet and slippery runways is incorporated in our computer program.

III. Mathematical Model of Landing Maneuver

A lumped-parameter mathematical model based on the laws of classical mechanics for a flat, nonrotating earth is presented [19–23,26,36]. Coriolis and transport acceleration is neglected ([21]) and inertial frame of reference is assumed. This will lead to a set of nonlinear coupled ODEs, which together with several nonlinear algebraic equations forms the complete zero-dimensional (lumped-parameter) mathematical model.

A. Model of Air Distance over Threshold

An airplane in a stabilized approach [1,9–11] crosses the threshold at a recommended TCH and at the reference airspeed v_{REF} (possibly plus wind additives) and continues steady descent until the flare height (FLH) [14]. The air distance covered between the TCH and the beginning of the flare at FLH is [19–23]:

$$s_{\text{AD}} = \frac{h_{\text{TCH}} - h_{\text{FLH}}}{\tan \gamma_{\text{APP}}} \approx \frac{h_{\text{TCH}} - h_{\text{FLH}}}{\gamma_{\text{APP}}} \tag{1}$$

Here, we assigned the threshold crossing height to the landing gear height. The cockpit and the glide slope antenna will cross the threshold at a higher TCH. This air distance is not a function of airspeed or ground speed, but depends only on the glide path angle and absolute heights provided the pilot is not ducking under on the approach. The airspeed of the airplane does not change appreciably in this portion of the flight [1,15]. The airspeed is not wind dependant, but the ground speed is:

$$v_{\text{GS}} = v_{\text{TAS}} \mp v_w = v_{\text{TAS}}\left(1 \mp \frac{v_w}{v_{\text{TAS}}}\right) = v_{\text{TAS}} \times \varsigma(v_{\text{TAS}}, v_w) \tag{2}$$

In Eq. (2), the negative sign applies to the headwind and the positive sign to the tailwind component. Knowing the ground-based glide path angle, one can calculate the required thrust-to-weight ratio for the power-on approach if the aerodynamic efficiency ($E = L/D$) in the landing configuration is known. We used the small glide path angle approximation and gave positive sign to the descent angle:

$$\tan \gamma_{\text{APP}} \approx \gamma_{\text{APP}} = ((D - T)/W)_{\text{APP}} = E^{-1} - (T/W) > 0 \tag{3}$$

Here, both the aerodynamic efficiency and the thrust-to-weight ratio are functions of the airspeed (or more precisely the AOA). In the case of headwind, the thrust-to-weight ratio will have to increase to maintain the aircraft on the glide path. The duration of the straight descent phase is therefore

$$t_{\text{AD}} = \frac{s_{\text{AD}}}{v_{\text{REF}}} \approx \frac{h_{\text{TCH}} - h_{\text{FLH}}}{\gamma \times v_{\text{REF}}} \tag{4}$$

The approach descent angle is usually between 2.75 and 3.25 deg, with 3 deg being the "normal" glide slope angle. It is a bad idea to

steepen the glide path in this phase of landing as the subsequent arrest of the vertical downward acceleration during the flare maneuver will be much harder for a transport-category airplane (large inertia) and may result in a bounce and/or hard landing. Too shallow or too steep descent angles can lead to an imprecise control of the touchdown point or hard landings, respectively. For example, if the airplane's aerodynamic efficiency in the landing configuration is $E = L/D = 8$ at the approach speed of 217 ft/s (130 kt or 66 m/s or 240 km/h), the T/W ratio and thrust required to maintain a 3 deg glide slope in no wind conditions and at $W = 135,000$ lb (B737-700) are 0.073 and 9855 lb (43.85 kN), respectively, or about 50% N_1 (fan speed) for each particular CFM-56 engine at sea level international standard atmosphere (ISA). We are neglecting the thrust variation with the airspeed, but we do include the effect of density altitude on the actual thrust produced [19,22,23].

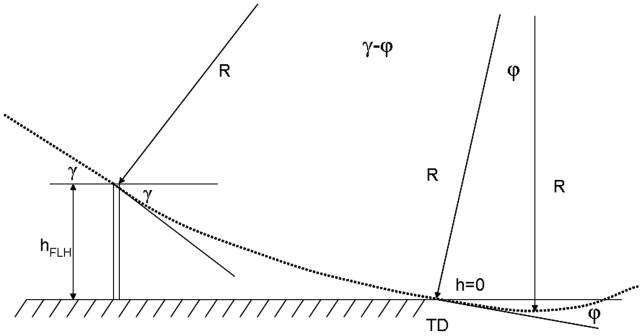

Fig. 2 Landing flare maneuver assuming constant flight load (not to scale).

B. Modeling of Landing Flare

The flare height is the altitude above the runway at which a pilot decides to start the rounding out maneuver by pitching up to arrest the descent rate. Coincidentally, the pilot is preventing the nose gear from striking the runway first. Simultaneously, the throttles are continuously and smoothly closed to idle. In Fig. 2, a schematic drawing of the landing flare is shown. The airplane's trajectory is represented by the dashed line. The aircraft impacts the runway at a small, but finite, angle. The descent rate at touchdown is not zero. During the landing flare transition, the AOA, α; pitch angle, θ; descent angle, γ; the vertical speed (ROD); and the horizontal (forward) airspeed of the airplane changes. Normally, the ground effect will become noticeable as the wing height above the ground becomes less than the half of the wing span.

The system of coupled nonlinear ODEs for the flare maneuver, together with the initial conditions and the appropriate algebraic relationships for the aerodynamic coefficients and other parameters, can be integrated numerically and the touchdown speed, flare time, and distance calculated. It is possible to analytically integrate the system of linearized ODEs by first adopting some rather severe assumptions and restrictions [16–18].

Such a fairly simplified analytical approach of tangential touchdown has been adopted by many authors [19–23]. However, such an approach is not capable of accounting for the many variations and strong nonlinearities that characterize the physical reality. The following coupled nonlinear ODEs, together with some algebraic relations, constitute the full mathematical model of the flare maneuver:

$$\dot{x} = v \times \cos\gamma \qquad \dot{h} = v \times \sin\gamma = \mathrm{ROD}(t)$$
$$\dot{v} = g\left\{\left[\frac{T(h)}{W}\right]_{\mathrm{FL}} \cos(\alpha+\delta) - \left[\frac{D_G(h)}{W}\right] - \sin\gamma\right\}$$
$$\approx g\left\{\left[\frac{T(h)}{W}\right]_{\mathrm{FL}} - \left[\frac{D_G(h)}{W}\right] - \sin\gamma\right\}$$
$$\dot{\gamma} = \frac{g}{v}\left\{\left[\frac{T(h)}{W}\right]_{\mathrm{FL}} \sin(\alpha+\delta) + n - \cos\gamma\right\} \approx \frac{g}{v}(n - \cos\gamma)$$
$$\dot{s} = v \pm v_w = v_{\mathrm{GS}} \qquad \dot{\alpha} = \dot{\theta} - \dot{\gamma} \qquad I_{yy} \times \ddot{\theta} = \mathcal{M} \qquad v = \sqrt{\dot{x}^2 + \dot{h}^2} \tag{5}$$

Ideally, the thrust throughout the flare is linearly decreasing to become idle at touchdown:

$$T(h) = \left[T_{\mathrm{APP}}(h/h_{\mathrm{FL}}) + T_{\mathrm{IDLE}}(1 - (h/h_{\mathrm{FL}}))\right]$$

Instead of solving the full system of differential equations describing flare, we will make use of some simplifying, yet reasonable, and experimentally verified assumptions. This is justified as the flare distance and elapsed time are shorter than the subsequent ground stopping roll. We are trying to maintain the same order of accuracy and level of uncertainty throughout the whole model. Our future study will focus on a full modeling of the flare dynamic equations. That will lead to a more accurate model, but the assumptions made here are conservative and err on the high side.

The flare height can be calculated from the operational requirement that the vertical velocity at touchdown be an arbitrarily and operationally acceptable small value. Coincidentally, the wheel impact angle will be small (half a degree or less):

$$h_{\mathrm{FL}} = R\cos\varphi - R\cos\gamma = R(\cos\varphi - \cos\gamma) \approx R\left(\frac{\gamma_{\mathrm{APP}}^2}{2} - \frac{\gamma_{\mathrm{TD}}^2}{2}\right)$$
$$= R\left(\frac{\gamma_{\mathrm{APP}}^2}{2} - \frac{\varphi^2}{2}\right) \tag{6}$$

where from Fig. 2 and trigonometric relationships it follows that the impact angle at which the main wheels touch down on the runway surface is

$$\gamma_{\mathrm{TD}} = \varphi = \frac{1}{v_{\mathrm{TD}}}\left|\left(\frac{\mathrm{d}h}{\mathrm{d}t}\right)\right|_{\mathrm{TD}}$$

Obviously, this angle should be very shallow and the corresponding vertical speed small enough to prevent large impact loads being transmitted to the landing gear assembly and the airplane structure. Touchdown vertical speeds in excess of 600 fpm could cause structural damage to the landing gear assembly.

The AOA and the C_L are increased due to the sustained increase of the airplane pitch angle resulting in a curved trajectory and changing γ. The radius of the flight load constant curved circular flare segment is calculated from the centripetal acceleration and the required increase in the lift force resulting in a curved path (gentle "zoom" maneuver):

$$R = \frac{v_{\mathrm{FL}}^2 \times \varsigma_{\mathrm{FL}}^2}{g(n_{\mathrm{FL}} - 1)} = \frac{2(W/S) \times \varsigma_{\mathrm{FL}}^2}{\rho g \Delta c_{L,\mathrm{FL}}} = \frac{v_{\mathrm{FL}}^2 \times \varsigma_{\mathrm{FL}}^2}{g}\frac{C_{L,\mathrm{FL}}}{\Delta C_{L,\mathrm{FL}}} \tag{7}$$

where the coefficient of lift and wind correction factor in flare are:

$$C_{L,\mathrm{FL}} = \frac{2(W/S)}{\rho v_{\mathrm{FL}}^2} \qquad \varsigma_{\mathrm{FL}} = \left(1 \mp \frac{v_w}{v_{\mathrm{FL}}}\right)$$

The increased lift coefficient obtained by the increasing AOA is necessary to increase the lift force, create vertical acceleration, slow down the descent rate, and produce a curved path in the vertical plane. The additional induced drag caused by the increasing AOA and changing gravity vector will result in a small deceleration. That deceleration will be offset by the decreasing induced drag as the airplane enters and descends through the ground effect. The flare height can be now expressed as

$$h_{\mathrm{FL}} = \frac{v_{\mathrm{FL}}^2 \times \varsigma_{\mathrm{FL}}^2 \times \gamma_{\mathrm{APP}}^2}{2g(n_{\mathrm{FL}} - 1)} - \frac{v_{\mathrm{FL}}^2 \times \varsigma_{\mathrm{FL}}^2}{2g(n_{\mathrm{FL}} - 1)}\left[\frac{1}{v_{\mathrm{TD}}}\left(\frac{\mathrm{d}h}{\mathrm{d}t}\right)_{\mathrm{TD}}\right]^2$$
$$= \frac{v_{\mathrm{FL}}^2 \times \varsigma_{\mathrm{FL}}^2}{2g(n_{\mathrm{FL}} - 1)}(\gamma_{\mathrm{APP}}^2 - \varphi^2) \tag{8}$$

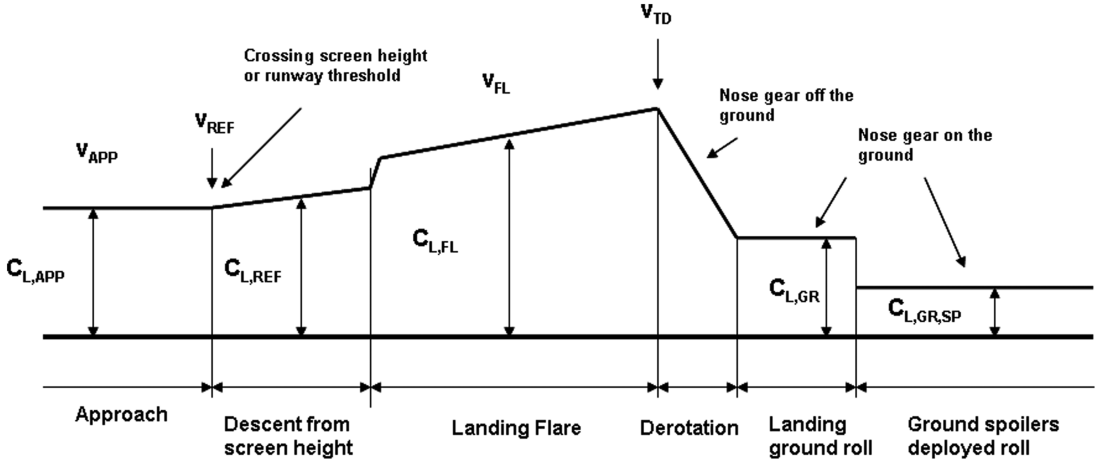

Fig. 3 Variation of lift coefficient throughout the landing (not to scale).

In Fig. 3, a variation of the lift coefficient throughout the landing maneuver is sketched (not to scale). The deployment of the lift-dump system leads to a significant reduction in the lift coefficient and, consequently, better braking efficiency.

The optimum flare height (in feet) for a $\gamma = 3$ deg approach angle, a constant normal flight load in flare of $n_{\mathrm{FL}} = 1.1$, and a ROD at touchdown not exceeding 1 fps (60 fpm) is

$$h^*_{\mathrm{FL}} = \frac{v^2_{\mathrm{FL}} \times \varsigma^2_{\mathrm{FL}}}{2g(n_{\mathrm{FL}} - 1)}(\gamma^2_{\mathrm{APP}} - \varphi^2) \approx \frac{v^2_{\mathrm{FLGS}} \times \gamma^2_{\mathrm{APP}}}{6.5} \approx \frac{(\mathrm{d}h/\mathrm{d}t)^2_{\mathrm{APP}}}{6.5} \quad (9)$$

where $(\mathrm{d}h/\mathrm{d}t)$ is the ROD (in ft/s) just before initiation of the flare maneuver. The pilot chooses the flare height visually and/or by radio altimeter (ground proximity warning system), and the required constant flight load in the flare is calculated from

$$n_{\mathrm{FL}} = 1 + \frac{v^2_{\mathrm{FL}} \times \varsigma^2_{\mathrm{FL}}}{2 \times g \times h_{\mathrm{FL}}}(\gamma^2_{\mathrm{APP}} - \varphi^2) \quad (10)$$

The common landing flare pitch-up rate ($\psi = \mathrm{d}\theta/\mathrm{d}t$) is usually between 0.5 and 1 deg/s ($n = 1.062$–1.124) for an airplane with a typical landing speed of 230 ft/s (70 m/s). The average airspeed in the flare is based on the threshold crossing speed, v_{REF}, plus wind additives. In this model, we assumed an average flare speed of 1.275 V_{so} and a touchdown speed of 1.25 V_{so} in a no-wind situation. Webb and Walker [15] reported touchdown speeds of 1.26 V_{so} (B737, A320, etc.). Blake and Elliott [1] mentioned only 5 kt of airspeed bleed off during the flare. Because an airplane can conduct an approach with excessive airspeed, we assumed a touchdown speed of 95% of the actual airspeed over the threshold. The average flare speed is thus 97.5% of the actual threshold crossing speed.

As shown in Fig. 4, the lift coefficient increases [19,21,22,26] in in-ground effect (IGE) for a given AOA, although the maximum lift coefficient and the stalling AOA is lower than in the outside ground effect (OGE). The pitching moment change in the ground effect often requires an additional gentle pullback pressure on the control column. Induced drag reduction and an increase in lift could result in airplane floating. Large aspect ratio and wing span aircraft, such as B747s, have such a massive ground effect that the pilot's pitch up input is quite small [12,14] and landings are smooth and uneventful.

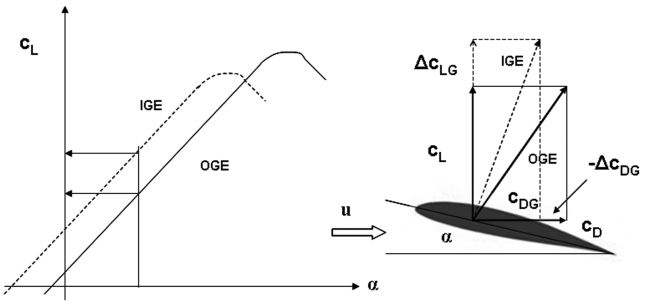

Fig. 4 Change of lift coefficient and aerodynamic forces in ground effect (not to scale).

The landing flare is an accelerated maneuver with the flight load, n, commonly in the range of 1.05–1.15 and with $n_{\mathrm{FL}} = 1.1$ being the "optimum" pitch rate (0.81 deg/s). The horizontal distance covered in the flare can be approximated as follows:

$$\begin{aligned} s_{\mathrm{FL}} &= R\sin(\gamma - \varphi) + t_{\mathrm{FLOAT}} v_{\mathrm{FL}} \varsigma_{\mathrm{FL}} \approx R(\gamma - \varphi) + t_{\mathrm{FLOAT}} v_{\mathrm{FL}} \varsigma_{\mathrm{FL}} \\ &= \frac{v^2_{\mathrm{FL}} \times \varsigma^2_{\mathrm{FL}}}{g(n_{\mathrm{FL}} - 1)}(\gamma_{\mathrm{APP}} - \varphi) \\ &\quad + v_{\mathrm{FL}} \times \varsigma_{\mathrm{FL}} \times t_{\mathrm{FLOAT}}\left(1 - 0.007\frac{t_{\mathrm{FLOAT}}}{2}\right) \end{aligned} \quad (11)$$

Here, float time accounts for the excessive floating, bouncing, or ballooning due to the improper flare technique. We assumed a slight deceleration in the float at an increasing AOA of 0.7% speed bleed off per second (200 ft float per 1 kt speed reduction) for a short-time approximation, which is consistent with the experience for a large-transport-category airplane [1,3,12,15]. This will occur when the zero sink is achieved just above the runway surface.

However, consistently shorter and safer landings will be achieved with a low, but finite, vertical speed at touchdown (<120 fpm or 2 fps). Differential equations of float can be derived from Eq. (5) and they yield

$$\begin{aligned} &\dot{x} = v \quad \dot{h} = 0 \quad \dot{v} = g\left\{\left[\frac{T(h)}{W}\right]_{\mathrm{FL}}\cos(\alpha + \delta) - \left[\frac{D_G(h)}{W}\right]\right\} \\ &\dot{\gamma} = \frac{g}{v}\left\{\left[\frac{T(h)}{W}\right]_{\mathrm{FL}}\sin(\alpha + \delta) + n - 1\right\} = 0 \quad \dot{s} = v \pm v_w = v_{\mathrm{GS}} \\ &\ddot{\alpha} = \ddot{\theta} \quad I_{yy} \times \ddot{\theta} = \mathcal{M} \end{aligned} \quad (12)$$

Equations (8), (11), and (12) put forward improvements over the previously developed models [16–23]. A tangential touchdown ("greaser" landing) is unrealistic and impossible to achieve with any consistency using conventional flight controls in any airplane. The time spent in flare is

$$t_{\mathrm{FL}} = \frac{s_{\mathrm{FL}}}{v_{\mathrm{FL}} \times \varsigma_{\mathrm{FL}}} = \frac{s_{\mathrm{FL}}}{v_{\mathrm{FLGS}}} \quad (13)$$

The time of flare (without float) can also be obtained using the small glide path angle approximation [in system equation (5)]:

$$\begin{aligned} &\frac{\mathrm{d}\gamma}{\mathrm{d}t} = \frac{g}{u_{\mathrm{FLGS}}}(n_{\mathrm{FL}} - 1) \\ &\Rightarrow \int_0^{t_{\mathrm{FL}}} \mathrm{d}t = \frac{\bar{v}_{\mathrm{FLGS}}}{g\Delta n_{\mathrm{FL}}}\int_{\gamma_{\mathrm{APP}}}^{\gamma_{\mathrm{TD}}} \mathrm{d}\gamma = \frac{\bar{v}_{\mathrm{FLGS}}(\gamma_{\mathrm{APP}} - \gamma_{\mathrm{TD}})}{g\Delta n_{\mathrm{FL}}} \end{aligned} \quad (14)$$

and integrating the glide path angle between γ_{APP} and γ_{TD}. The total air distance and elapsed time is the sum of the distances and time covered in a straight descent over the threshold and the horizontal distance and time covered in a curved flare:

$$s_A = s_{AD} + s_{FL}, \qquad t_A = t_{AD} + t_{FL}$$

The touchdown speed, elapsed time, and distance covered can be calculated by the numerical integration of the full set of nonlinear ODE or estimated from the law of conservation of energy in flare transition [16,22]:

$$\frac{\mathrm{d}}{\mathrm{d}t}\left(\frac{v^2}{2g}\right) + \frac{\mathrm{d}h}{\mathrm{d}t} = \frac{[T(h)\cos(\alpha+\delta) - D_G(h)]u}{W} \approx \frac{[T(h) - D_G(h)]}{W}\frac{\mathrm{d}s}{\mathrm{d}t} \tag{15}$$

This equation can be integrated by employing a few assumptions, such as the assumption that the thrust decreases linearly to flight idle while the aerodynamic efficiency increases somewhat throughout the flare maneuver. The balance of forces will yield the correct touchdown speed.

The pitch up in flare should be about 0.8 deg/s, which results in a gentle flight load of $n_{FL} = 1.1$ for a typical approach and flare speeds of large-transport-category airplanes. It takes about 3–5 s to pitch up from the typical 2–3 deg nose up in the v_{REF} approach configuration to the touchdown attitude of, typically, 4–6 deg nose up [1,12,14,15].

Thus, a typical large-transport-category airplane will cross the threshold at a 35–50 ft gear height at speeds between 200–250 ft/s (61–76 m/s). It will cover 600–800 ft (180–245 m) in 3–4 s until the flare maneuver at about 20–30 ft, and touchdown will occur in another 3–4 s. The touchdown ROD should be no more than 120 fpm (0.6 m/s) while covering additional 500–700 ft during flare. Ideally, the total distance to touchdown is between 1000 ft (300 m) and 1500 ft (460 m) and 5–8 s after crossing the runway threshold.

C. Ground Roll Flight Regime

The landing ground roll consists of two phases. After the touchdown on the main wheels, a particular distance is covered before the nose gear is derotated. After all the tires are on the ground, the full braking effort can take place. Usually, there is a delay in thrust reverser deployment due to the mechanic interlocking mechanism, which prevents thrust increase before the clamshells, buckets, or cascades are locked in proper position. There is also an additional lag due to engine spool up from ground idle. Full friction braking using an antiskid system, in conjunction with the ground spoilers' deployment, can start soon after all wheels are on the runway and rotating at a predetermined speed. An automatic braking mechanism is often used. Such a braking system has predetermined deceleration rates (e.g., 10, 7, or 4 ft/s^2), runway conditions permitting. The hard application of brakes before the nose gear is on the runway can cause rapid pitch down acceleration and a damaging ground impact on the nose gear. In Fig. 5, the schedule of various braking mechanisms during the ground roll is shown schematically. Normally, the reverse thrust is retarded to reverse ground idle by about 60 knots indicated airspeed (KIAS) but, in an emergency, it can be used until stop (e.g., in the B747-200 Royal Air Maroc overrun accident). Ground spoilers are normally deployed between the main gear and the nose gear touchdown when in automode. The deployment of various motion-retarding devices and other events is simulated using the Heaviside step functions.

The ODEs that describe the motion of the aircraft on the ground are based on Newton's second law for flat and nonrotating earth. The major deceleration forces acting on an airplane are the braking force on the main wheels, rolling friction of the nose gear, reverse thrust from the engines (not required for certification), aerodynamic drag, and possibly the effect of a positive runway slope (uphill). Downhill slope increases ground roll. Headwind reduces the landing distance. The adverse effect of tailwind is especially worrying. Title 14, CFR 25.175 requires that no more than 50% of the headwind and not less than 150% of the tailwind may be used for DLDR estimation by individual operators. In all cases, the braking friction provided by the brakes on the main wheels provides the dominant stopping force on dry runways. In the case of slick and slippery runways, thrust reversing becomes central.

1. *Derotation of the Nose Gear*

When the main gears touch down, the nose gear should be still in the air. Derotation is usually commenced with a negative pitch rate of about 2 deg/s, which avoids slamming the nose gear on the runway or derotating too slowly and wasting usable runway [2,3,10–12,14,15].

During derotation, the rolling friction on the main tires and the aerodynamic drag are working on slowing down the airplane. An idle thrust and downhill runway will accelerate the aircraft. During the typical 3 s of derotation, the forward speed will remain practically unchanged. Mair and Birdsall [20] reported a speed reduction of only 1.5% per second if brakes are not used in the derotation regime for a typical transport-category aircraft. For a 130 kt touchdown ground speed and a 3 s derotation, the ground speed decreases by less than 6 kt, which is consistent with the operational experience and a fact that we used in our model. The differential momentum equation can be written for the decreasing pitch angle and AOA, resulting in a changing drag, lift, normal reaction, and braking force for the nose gear derotation ground roll phase:

$$\frac{1}{g}\dot{v} = \left(\frac{T}{W}\right)_{\text{idle}} - \frac{D_G}{W} - \mu_R\left(\frac{N_M}{W}\right) \mp \sin\phi$$
$$L_G + N_M = W\cos\phi \approx W \qquad \dot{s} = v \pm v_w \tag{16}$$
$$\dot{W} = -\text{TSFC} \times T \approx 0 \qquad v(t=0) = v_{TD} \qquad s(t=0) = 0$$

A common practice in previous studies was to assume that the ground speed stays constant during the derotation phase [22]. However, we are including a small deceleration according to a semi-empirical model and observations made by Mair and Birdsall [20], resulting in a speed bleed off:

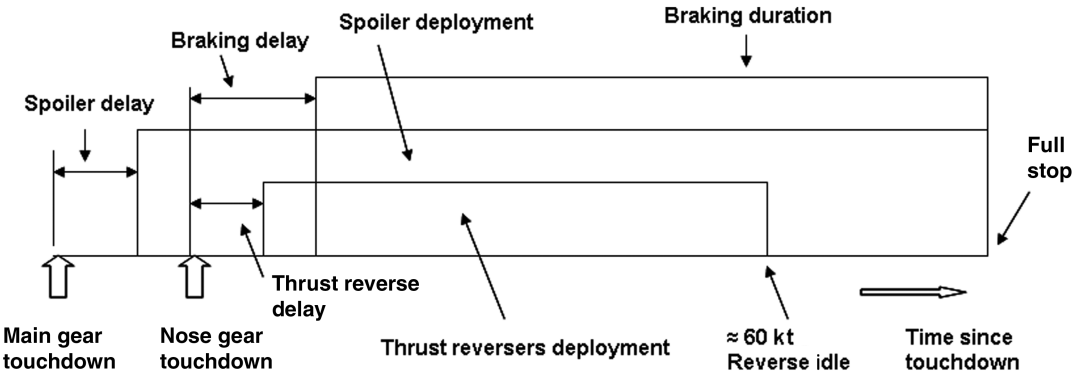

Fig. 5 Schedule of ground and flight spoilers (lift-dump system), friction braking, and thrust reverser deployment and restowing (not to scale).

$$v_{\mathrm{NGUP}}(t) = v_{\mathrm{TD}} \times \varsigma_{\mathrm{FL}}(1 - 0.015 \times t) = \frac{\mathrm{d}s}{\mathrm{d}t} \tag{17}$$

The distance covered during this phase is

$$s_{\mathrm{NGUP}} = v_{\mathrm{TD}} \times \varsigma_{\mathrm{FL}} \times t_{\mathrm{NGUP}}(1\text{–}0.015 \times (t_{\mathrm{NGUP}}/2)) \tag{18}$$

where t_{NGUP} is the number of seconds required for the nose gear to be lowered to the ground and is determined by the pilot's action. Usually this is taken to be 3 s.

2. Ground Roll with All Wheels on Runway

The equations of motion for the ground roll with all tires firmly on the ground are

$$\begin{aligned} &\frac{W}{g}\dot{v} = -T_{\mathrm{REV}} - D_G - \mu_{\mathrm{RB}}N_M - \mu_R N_N \mp W\sin\phi \\ &L_G + N_M + N_N = W\cos\phi \approx W \qquad \dot{s} = v \pm v_w \\ &\dot{W} = -\mathrm{TSFC} \times T \qquad v(0) = v_{\mathrm{NGTD}} \qquad s(0) = 0 \\ &W(0) = LW \end{aligned} \tag{19}$$

The forces N_N and N_M are the normal reaction forces on the nose- and main-wheel trucks. We are neglecting any effect of the contamination drag (e.g., slush, deeper snow, etc.) as it would only reduce the landing ground roll distance. Any lift force developing on the wing decreases the normal reaction force and, accordingly, the rolling and braking friction force. Because the runway inclination angle (gradient) for large-transport-category airplanes is usually very small, on the order of 1–2%, one can write the momentum equation in terms of g units:

$$\frac{1}{g}\frac{\mathrm{d}v}{\mathrm{d}t} = \left\{-\left(\frac{T}{W}\right)_{\mathrm{REV}} - \left(\frac{D_G - \mu_{\mathrm{RB}}L_G}{W}\right) + \frac{N_N}{W}(\mu_{\mathrm{RB}} - \mu_R) - (\mu_{\mathrm{RB}} \pm \phi)\right\} = \frac{a_G(t)}{g} \tag{20}$$

If the expressions for drag and lift, which must be evaluated with ground effect in mind, are now substituted into Eq. (20), one obtains

$$\begin{aligned} &\frac{1}{g}\dot{v} = \left[-\left(\frac{T}{W}\right)_{\mathrm{REV}} - (\mu_{\mathrm{RB}} \pm \phi) + \frac{N_N}{W}(\mu_{\mathrm{RB}} - \mu_R)\right] \\ &\quad - \frac{C_{D,G} - \mu_{\mathrm{RB}}C_{L,G}}{(W/S)}\frac{\rho}{2}v^2 = \frac{a_G(t)}{g} \\ &\dot{s} = v \pm v_w = v \times \varsigma \qquad \dot{W} = -\mathrm{TSFC} \times T \approx 0 \\ &v(t=0) = v_{\mathrm{NGTD}} \qquad s(t=0) = 0 \qquad W(t=0) = LW \end{aligned} \tag{21}$$

which, with the following algebraic relationships [17–23,36], forms the complete mathematical model of the ground roll:

$$\begin{aligned} &D_G(h) = \frac{1}{2}\rho \times v^2 \times S \times C_{DG}(h) \\ &C_{DG}(h) = C_{D,0} + \Delta C_{D,0} + \left[k_1 + \frac{G(h)}{\pi \times e \times AR}\right]C_L^2 \\ &G(h) = \frac{(16 \times h/b)^2}{1 + (16 \times h/b)^2} \quad \Delta C_{D,0} = \left(2.42\frac{W}{S}\right)K_{uc}\left(\frac{W}{2.2}\right)^{-0.215} \\ &k_1 = 0.02 \end{aligned} \tag{22}$$

where K_{uc} is a function of flap position, according to Mair and Birdsall [20]. We assumed the normal reaction force of the nose gear to be about 8% of the aircraft weight [22]. In general, the reaction force on the nose gear can be calculated from the balance of forces and moments. The idle thrust value (when not in reverse) was also used in all computations. In addition, it is quite justifiable to neglect small weight loss during landing rollout. The thrust-specific fuel consumption is on the order of 0.5 lb/hr of fuel per each pound of thrust produced for modern turbofan designs at lower altitudes. This ground roll usually takes no longer than 30 s and the weight loss is thus less than 0.2% with maximum reversers, which causes an insignificant reactive force.

IV. Methods and Materials

A program written in MATLAB® programming language has been developed that takes all the atmospheric, meteorological, aircraft, and airport specific inputs and calculates the deceleration, speed, and distance histories for the complete landing regime. Because of many uncertainties in the aircraft aerodynamic data, we estimated the total uncertainty of distance predictions to be about 100 ft in DLDR (60 ft in DLD) based on the certification tests on the Boeing 737-800. This uncertainty analysis will be shown later. The atmospheric data use the ISA equations to determine the standard temperature, density, and pressure for any given environmental conditions [19–23].

A. Simulation Program

The core ODE solver is a "homemade" marching-in-time modified-Euler or Heun's predictor-corrector method employed to solve the system of nonlinear coupled ODEs. This method is also analogous to Runge–Kutta's second order and consists of the Euler predictor with the trapezoidal corrector [37]. The slope is calculated simultaneously at both ends of the desired time interval, Δt, for all ODEs, and the average slopes are just the arithmetic means of the two boundary slopes at each time interval. The time step was changed between 0.1 and 0.025 s and no noticeable change in integrated values was found. The stopping criterion used is for the ground speed to fall below 0.2 kt. At the same time, the true airspeed (TAS) was evaluated against the wind velocity and the relative error had to be less than 2%. When the ground speed is zero, the TAS is equal to the wind speed component along the aircraft's longitudinal axis. Therefore, this was a sufficiently good check of the integration accuracy and consistency. In general, the fidelity of the model is questionable below ground speeds of 2–3 kt, due to the strongly nonlinear nature of the rolling-friction coefficient for a small tire slip. The very last tire movement changes from rolling to skidding. However, at such small ground speeds, only very small errors in integrated velocities or distances exist. The step (Heaviside) functions have been used (Fig. 5) to simulate various deceleration systems. The inertia of deployment and redeployment is thus neglected. Once the integration was performed and the speed and the distance of the ground run part were estimated, it was possible to plot all the time-deceleration-speed-distance histories.

The rolling-friction coefficients with or without braking were calculated as a decreasing linear function of ground speed using the correlations obtained from transport-category-aircraft testing [24,25,33–35]:

$$\mu = \mu_o - (\mu_o - \mu_1)(v_{\mathrm{GS}}/100) \tag{23}$$

where the ground speed is in knots, and μ_0 and μ_1 are measured values [25] at almost 0 and 100 kt, respectively. Above 100 kt, the rolling-friction coefficient is fixed at 0.03 for flooded and iced-up runways [25]. For other runway contaminations, the friction coefficient can be extrapolated for higher speeds. We do not distinguish between the two-, four-, or six-wheel trucks (e.g., the Boeing 777). In reality, the wheels rolling behind the front wheels will have a somewhat lower rolling coefficient of friction.

It is worth reiterating that Croll and Martin [24] were unable to obtain consistent μ vs v relationships. They were using a French-made Dassault Falcon 20 corporate jet aircraft. In this study, the Canadian runway friction index [24] was calculated from the rolling-friction data. The experimental results obtained by Yager [25] employing NASA's B737-100 research aircraft were used in our program as the core data for the surface- and speed-dependent rolling friction.

A very hazardous event is trying to stop an aircraft that is hydroplaning. This is a phenomenon in which the tires are lifted off the runway surface, resulting in a vanishingly small braking

efficiency. Hydroplaning can be dynamic, viscous, or reverted rubber. Extensive research has been conducted on the hydroplaning mechanism, and a summary of it can be found in Lowery [3], Davis [12], and Horne [33]. On flooded runways with at least 6–10 mm of stagnant liquid film, tires may be lifted off the runway surface and slide due to the hydrodynamic normal pressure, resulting in a very low friction coefficient, the loss of directional control, and diminishing tire rotation (no antiskid function). Brakes should never be applied before there is confirmation of the tire rotation and a positive load on landing gears. Hydroplaning speeds for rotating and nonrotating tires are, respectively, [33]

$$v_{\mathrm{HP}}^{r} = 9\sqrt{p_{\mathrm{tires}}} \qquad v_{\mathrm{HP}}^{nr} = 7.1\sqrt{p_{\mathrm{tires}}} \tag{24}$$

Many autobrake systems will have a time delay and/or a required tire rotation speed verified before the antiskid braking commences. It is clear that if there is no tire rotation on a slick or hydroplaning surface, the low friction coefficient will prevail over a larger speed range and time and dramatically increase the landing distance. For the Boeing 737 series (two-wheel truck), we used the nose and main tire pressure of 148 psi (about 10 bar). We also investigated the effect of the brake energy limit and tire speed limitation. These two effects are really only important in the rare case of a zero-flap landing.

The total landing distance and the total elapsed time, which includes both the air and the ground roll, are

$$s_{\mathrm{LD}} = s_A + s_{\mathrm{NGUP}} + s_{\mathrm{GR}} \qquad t_{\mathrm{LD}} = t_A + t_{\mathrm{NGUP}} + t_{\mathrm{GR}} \tag{25}$$

The statistical FAA method of calculating landing distance [22] was also used to compare the actual landing requirements with the FAA-mandated distances:

$$\mathrm{DLDR} = 0.3 \times v_{\mathrm{APP}}^2 = 0.3(1.3 \times v_{\mathrm{so}})^2 = 0.507 \times v_{\mathrm{so}}^2$$

The approach and stalling speed in the landing configuration is expressed in knots true airspeed. Some of the special features of our simulation program are as follows:

1) Braking strength can be adjusted in several discrete steps from 0 to 100%.

2) Reverse-thrust intensity can be set in several discrete steps from 0 to 100%.

3) The calibrated/indicated airspeed, at which the idle reverse is commanded, can be chosen as desired.

4) Great flexibility exists in choosing time delays for the deployment of various deceleration devices (brakes, lift-dump system, and thrust reversers).

5) The program calculates the optimum flare height.

6) The program is capable of simulating bouncing, ballooning, and floating.

7) The ability to linearly change the rolling-friction coefficient based on experimental data for many types of runway conditions is included.

8) Hydroplaning conditions on nongrooved wet and flooded runways can be simulated, and the accompanying friction coefficient calculated.

The model was extensively tested and compared, whenever possible, with the existing analytical solutions [19–23] and the experimental data. Various scenarios of use, or nonuse, of braking devices were tested to verify the logic and the robustness of the program. The program performed very well and is quite fast. Typically, it takes about 2–3 s to compute the solution and an additional 2–3 s to generate the plots.

B. Verification of Model

Every mathematical model introduces errors and uncertainties due to the approximations and assumptions made when modeling the real physical world. In addition, truncation and the rounding-off errors are introduced when executing the coded program on a digital computer. To investigate analytically the overall uncertainty of our model would be a tremendous task that we will leave for the future study. Therefore, we base our uncertainty claim of 100 ft on the comparison of the certification aircraft landing distance tests and our simulations under equivalent conditions. It is impossible to recreate all the details from the real world, but the landing certification runs provide a highly controlled environment that is very useful for our model validation. We have used Boeing's original data, FAR's landing runway length requirements, which already include the safety factor of 167% for the dry runway.

The conditions for the Boeing 737-800 FAA dry-landing runway length (DLDR) certifications are a standard day, autospoilers operative, antiskid operative, zero wind, and flaps at 40 deg. Additional conditions not specifically mentioned are a zero-gradient runway, crossing threshold at reference airspeed, gear height of 50 ft, no thrust reversing, 3 s to lower the nose gear, and maximum braking effort. Also, the antiskid brake delay after the nose gear touchdown is 1 s. In Table 1, we summarize the results of the landing runs of the current production Boeing 737-800 without winglets (with a maximum landing weight, or MLW, of 144,000 lb) and the simulations using our model at different landing weights and density altitudes.

From Table 1 we may conclude that the model's maximum uncertainty is no larger than 100 ft for the domain of our computations. This actually means that the simulation and experimental data are within a maximum uncertainty of 60 ft only. The difference of 40 ft comes from the FAA safety factor, which also amplifies uncertainty. These results are quite impressive. It also shows that the assumptions made here were quite reasonable. Of course, one can spend a lot of time refining certain details, but often that extra effort is not rewarded with a significantly decreased uncertainty.

However, our claim of a maximum 100 ft uncertainty cannot be absolute for any density altitude and weight for a specific airplane. Also, the model will have to be tested to establish the uncertainty limits for other aircraft models. However, the fundamental physics of the landing maneuver were captured adequately. The rms value of the uncertainty will be, of course, smaller than 100 ft (or 60 ft) for the range of weights and density altitudes that we used here.

It is important to note that the DLDR is extremely sensitive on the main gear touchdown point location. In our simulation, we

Table 1 Comparison of DLDR between the original Boeing 737-800 (no winglets) landing data and the simulation results for different weights and density altitudes. Maximum effort antiskid braking and autospoiler operation were simulated. Thrust reversing was not used and the aircraft crossed threshold at reference airspeed

Landing weight, lb	Density altitude, ft	DLDR Boeing, ft	DLDR simulation, ft	Difference	
				Ft	%
144,000	Sea level	5380	5432	+52	+0.97
	4000	5890	5795	−95	−1.61
140,000	Sea level	5230	5291	+61	+1.17
	4000	5710	5658	−51	−0.89
135,000	Sea level	5025	5120	+95	+1.86
	4000	5510	5442	−68	−1.23
130,000	Sea level	4820	4902	+82	+2.90
	4000	5310	5254	−56	−1.05

maintained the same sustained control column pull of 1.09 g, whereas the flare height had to be modulated with the density altitude and the weight changes to achieve the consistent 120 fpm touchdown vertical speed. We were adjusting the free flare parameters so that the airplane always touches down at around 1200 ft from the runway threshold. Even small deviations in the rate of flare pitch up and the choice of flare height could easily increase the touchdown point by 200–300 ft, which, with the FAA factor of 167%, results in an additional 330–500 ft of required runway length. It is impossible, with any consistency, in daily airline operations to replicate a test pilot's aggressive certification landing tests, which are performed in a highly controlled, disciplined, and systematic environment.

V. Simulation Results

It is impractical to simulate all the possible combinations and scenarios of adverse landing conditions and contaminated runways and present it in a textual or graphic form. We have to restrict ourselves here to a few critical cases that are sometimes encountered in practice. We will focus on some of the more serious adverse conditions, which, if they occur simultaneously with the runway contamination, can result in a landing accident.

Typical runway surface conditions are dry asphalt/concrete; wet asphalt/concrete (grooved and nongrooved surfaces); slush asphalt/concrete; fresh, loose, or packed snow on asphalt/concrete; and thin ice on asphalt/concrete. Various adverse conditions are the effect of density altitude, the effect of wind (tailwind, headwind, or crosswind), zero-flap landing, antiskid and/or brake system malfunction, spoiler deployment delay (mechanical, pilot technique), thrust reversers deployment time delay (mechanical, pilot technique), the effect of being high over the threshold (piloting technique), the effect of being fast over the threshold and at touchdown (pilot technique), bouncing and ballooning with excessive floating (pilot technique), skid development, and hydroplaning.

A particularly problematic situation occurs when one or more adverse conditions are taking place simultaneously with the runway contamination. An extreme scenario would be landing with zero flaps and tailwind on a wet or icy runway. However, as real-life experience shows, the conditions do not have to be that extreme. Combined with improper pilot performance, sometimes small adverse conditions multiply, resulting in a landing overrun [6,7,10,11,14,15].

One rather optimistic landing scenario that is every pilot's dream consists of a dry runway, a headwind, the correct threshold speed and height, a new airplane and brakes, a long runway, etc. The opposite extreme would be every pilot's nightmare, that is, a slick/slippery runway, a tailwind and/or crosswind, going too fast and being too high over the runway threshold, windshear and turbulence on the final approach, a short runway, excessive delay on thrust reversing, the ground spoilers not autodeployed, etc. Although it sounds improbable, such a nightmarish scenario actually happened to the crew of the aforementioned American Airlines flight 1420 [27].

To compare the required landing distances and times for dry and contaminated runways, we used a Boeing 737-800 at a MLW of 144,000 lb. The following conditions were also assumed: reference speed plus 5 kt (minimum wind additive), where the reference speed, v_{REF}, is 142 KIAS; full landing flaps and slats; a 3 deg glide path angle; a density altitude of 4000 ft; a maximum braking antiskid effort; a full reverse thrust; a headwind of 10 kt; a gear TCH of 40 ft; a flare height of 24 ft; a load factor in flare constant at 1.1 g; no float; 3 s to lower the nose gear; 0 s in spoiler delay; 3 s in reverse-thrust delay; and a 5 s delay in maximum braking effort after the nose gear touchdown. Furthermore, the idle reverse was commanded at 60 KIAS, the runway average downhill slope was 1%, and a 7000-ft-long runway was used.

In Table 2, the results for a dry runway and runways with various contaminants are summarized. In all instances, the air distance to main gear touchdown is 1115 ft and the time elapsed from TCH is 4.64 s. Main gear touchdown occurred at 138 kt and the nose gear touched down 3 s later at the ground speed of 132 kt, during which time the airplane consumed additional 653 ft of runway. The ROD at touchdown was a firm and safe 96 fpm (1.6 fps) and the total distance (air plus ground) to stop was 3496 ft for the dry runway. The FAA required landing distance (from Boeing data) is 5890 ft for a dry runway and 6774 ft for a wet-factored runway. These are zero-wind values. Using the FAA mandated 50% of headwind distance correction (Title 14, CFR 25) would result in a slightly shorter DLDR and WLDR. The LDA of 7000 ft should then be quite satisfactory in both cases. In Fig. 6, the simulation results for a dry runway and the aforementioned conditions are shown.

The simulation results summarized in Table 2 also show that a B737-800 on a thin-ice-covered runway would require 5549 ft to stop, that is, a 58.7% longer total landing distance or an 86.3% longer ground roll. The full time history of the speeds, distances, and decelerations for a thin-ice-contaminated runway is shown in Fig. 7. Quite clearly, for icy runways, the main retarding force is the reverse thrust, which delivers on average a 2–3 times higher deceleration than the friction braking. A downhill slope of −1% provides negligible forward acceleration. Aerodynamic braking is fairly insignificant for dry runways, but somewhat important for low-friction surfaces. In the first part of the ground roll, aerodynamic drag is the dominant, yet absolutely weak, retarding force until the ground spoilers, thrust reversers, and brakes become effective. In the case of the runway covered with thin ice, thrust reversing provides about 70%, aerodynamic friction 20%, and friction braking only 10% of the total retarding force at the ground speed of 120 kt. Of course, in the case of emergency stopping, the pilot is expected to keep the maximum reverse thrust until the airplane is fully stopped. Some of the surfaces, such as the wet and flooded nongrooved runways, will induce hydroplaning, which, in the case of B737-800s, is about 109.5 kt with tires rotating.

In analyzing the simulation results from Table 2, one might conclude that the FAA required safety factor for the wet runway would always be adequate for any runway contamination. In a way, the FAA lumps any runway contamination in a wet-runway category as far as the safety factor is concerned. The safety factor for a dry or wet runway would by no means always protect the airplane from running over the end. As we will see later, some minor operational errors combined with the contaminated runway could easily send the airplane over the edge.

In Fig. 8, the second scenario for the 7000 ft runway contaminated with thin ice is presented. The gear TCH was 50 ft, the airplane was on reference speed plus 20 kt, and no wind was present. Because the wind is zero, the same WLDR of 6774 ft is required. The flare height was 33 ft to achieve a firm 148 fpm touchdown. The total air distance until touchdown is an acceptable 1400 ft, and 4.93 s elapsed since the threshold crossing. All other data are the same as in the previous example (Fig. 7). So how did the airplane do?

The airplane skidded off the runway end 43 s after crossing the threshold at a ground speed of 32 kt. Once out of runway, the

Table 2 Landing distances, percentage distance increase, and time to stop over a dry runway from TCH to full stop for a Boeing 737-800 at the MLW and conditions listed. Maximum effort braking and thrust reversing until 60 KIAS is assumed (followed by idle reverse)

Runway	Dry	Wet grooved	Wet nongrooved	Flooded nongrooved	Slush	Dry loose snow (0.5–3 in.)	Packed snow	Thin ice
Total landing distance, ±100 ft	3496	3543	4177	4473	3896	4671	4377	5549
Percent increase distance, %	0	1.33	19.5	27.9	11.4	33.6	25.2	58.7
Time, ±0.67 s	19.9	20.7	25.4	30.0	23.4	36.8	29.0	47.5

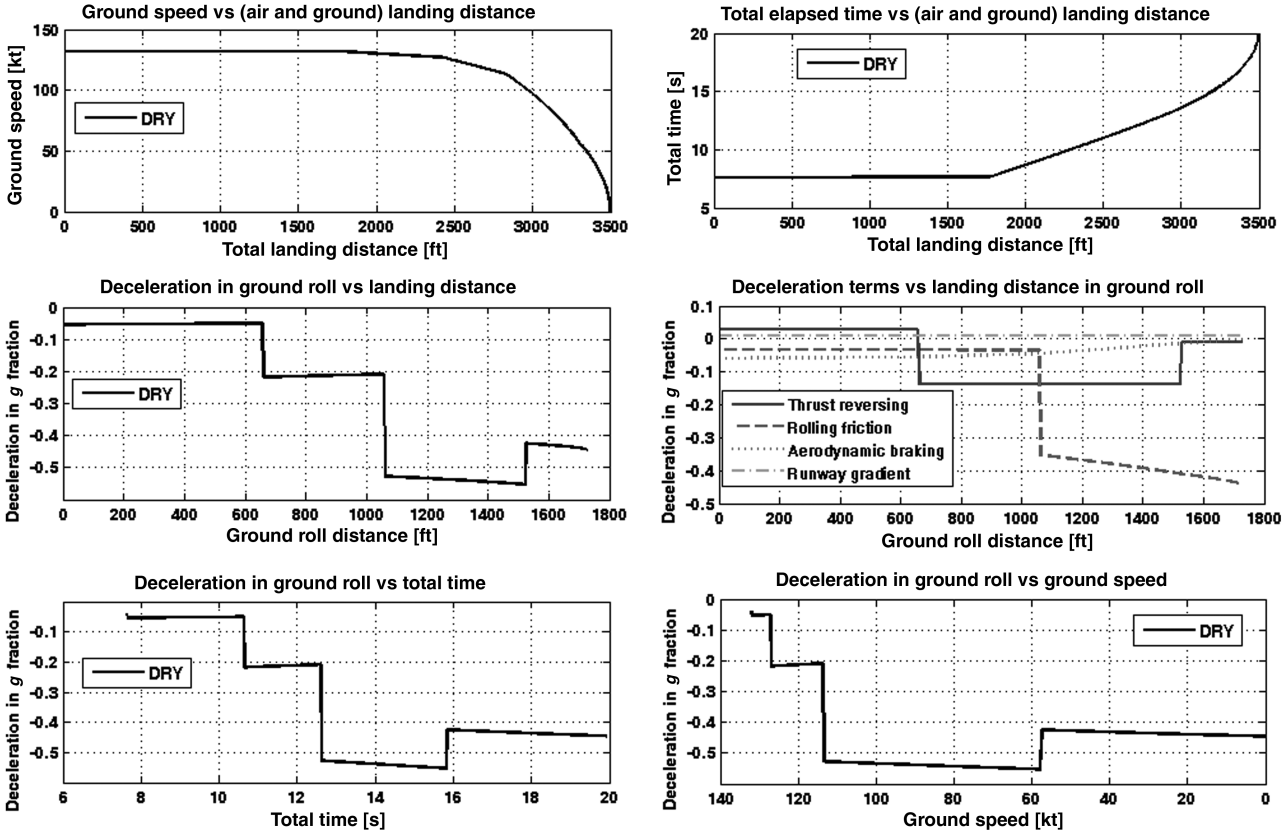

Fig. 6 Boeing 737-800 at 144,000 lb landing on a dry runway.

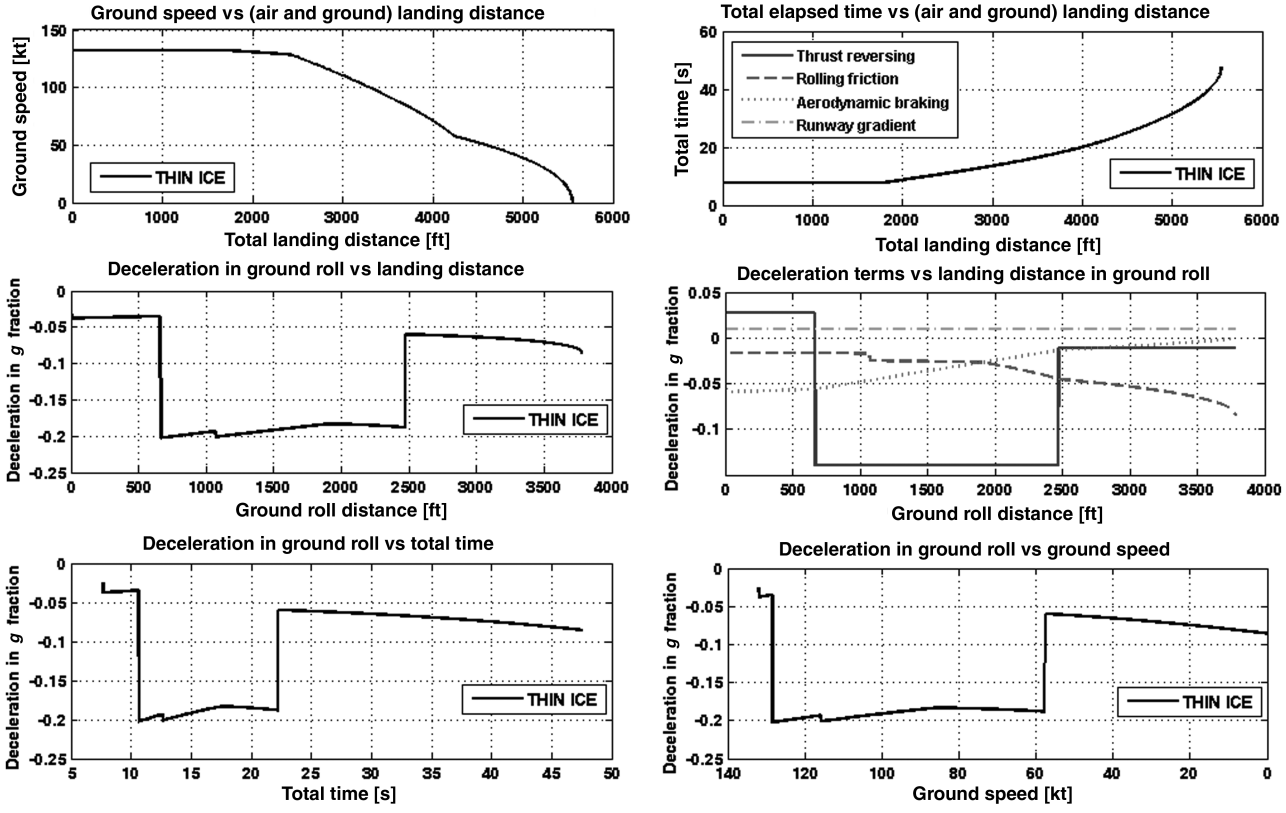

Fig. 7 Boeing 737-800 at 144,000 lb landing on iced-up runway.

stopping distance and deceleration forces are difficult to estimate, but certainly they are going to lead to significant damage and possibly fatalities/injuries considering the residual kinetic energy. Sometimes, a special EMAS is installed at the runway ends to provide high deceleration forces. However, such a solution is not always practical or possible. Actually, the only operational error the pilot committed was to cross the threshold a bit fast. However, up to 20 KIAS wind add on is allowed per SOP to account for gusty and/or steady winds.

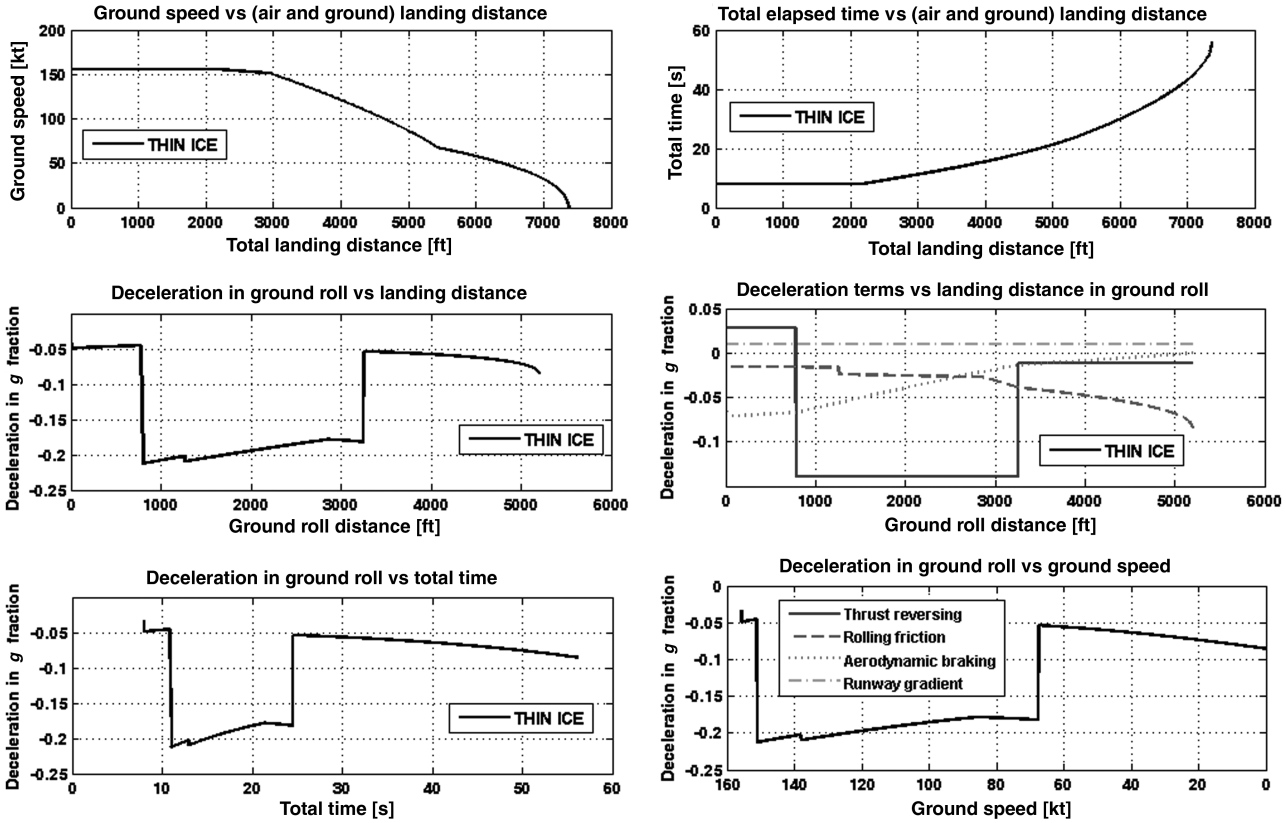

Fig. 8 Boeing 737-800 at 144,000 lb landing on iced-up runway. The threshold crossing height is 50 ft, zero wind, and 20 kt faster than the reference speed.

Theoretically, the airplane needed 7369 ft to stop in 56 s. However, the runway was only 7000 ft long.

Let us now analyze another, even more drastic case. The runway is covered with thin ice, the gear TCH is 80 ft, the airplane is on reference speed plus 20 kt, and there is a 10 kt tailwind. The total air distance until touchdown is a tolerable 1950 ft, and 6.45 s have elapsed since the threshold crossing. As expected, the airplane skidded off the end of the 7000-ft-long runway at a ground speed of 68.3 kt and 31.8 s after threshold crossing. This time, the airplane came 30 ft higher and 20 kt faster. Up to 10 kt of tailwind is an acceptable upper limit by many airline operators, but the 150% correction for the tailwind must be incorporated into the required landing distance by CFR 25.125, that is, the effective tailwind component will be at least 15 kt. Different operators might have different wind corrections, but in most cases the WLDR will be about 8000 ft. Theoretically, the airplane needed 9073 ft to stop in 65 s.

Interestingly, a repeated simulation showed that, even if the airplane crossed the threshold at 40 ft (saving about 200 ft of runway) and started the maximum antiskid braking effort within 1 s of the nose gear touchdown, the 8000-ft-long runway would still not have been enough. The airplane would have skidded off the runway end at 32.6 kt, still a substantial speed. Clearly, the FAA required wet-runway-factored landing distance may not always suffice.

VI. Discussion of Results

If the ground speed at touchdown and the average deceleration in ground roll are known, the ground stopping distance is simply

$$s_{GR} = \frac{v_{TD}^2 \times W}{2 \times g \times \bar{F}_{net}} = \frac{v_{TD}^2}{2 \times \bar{a}_{GR}} \tag{26}$$

The effect of the touchdown speed and the average deceleration can be estimated for small changes about the nominal condition from

$$\frac{\Delta s_{GR}}{s_{GR}} = \frac{2 \times \Delta v_{TD}}{v_{TD}} - \frac{\Delta \bar{a}_{GR}}{\bar{a}_{GR}} \tag{27}$$

Naively, one could conclude that the effect of the touchdown ground speed is more important in determining the landing distance, as it carries twice the weight. However, the average deceleration in the ground roll can vary by an order of magnitude (from dry to icy or hydroplaning conditions). The touchdown speed never varies by more than 40% of the reference speed for a given airplane at a certain weight, and then only in the extreme case of zero-flap landing. Usually, the airspeed increment in normal operations is no more than 10–16%, requiring at most a 35% increase in the ground roll. On the other hand, the deceleration can be easily quartered compared with the dry runway. In that case, the ground roll distance would quadruple according to Eq. (22). If we look back and compare the results from Figs. 6 and 7, we will see that the maximum deceleration for the dry runway is about 0.55 g and the average is 10.7 ft/s^2, whereas for the iced runway those numbers are 0.2 g and 3.3 ft/s^2, respectively. This would be a factor of 3.2. The ground rolls are 2377 and 4434 ft for a dry and an icy runway, respectively, which is a factor of 1.86. Let us not forget that the analysis using Eq. (22) is linear and strictly valid for small perturbations only. Instantaneous and average deceleration could be measured using accelerometers or numerically integrated by knowing the time history of all forces and masses involved.

Also, the air distance has to be added to the ground roll. An inaccurate touchdown point may lead to a landing overrun, regardless of the braking technique. We estimated a maximum uncertainty in the calculated landing distance of 100 ft for the range of weights and density altitudes in a B737-800. However, it would be desirable to compare our computational results with regular daily aircraft operations to verify the accuracy of the deployment of simulated retarding devices. Kimberlin [38]) highlighted some experimental methods and data analysis used in measuring landing and takeoff performance.

In practice, there is often a serious problem with runways for which the braking action can be reported or measured as "good" for the first half or two-thirds of the runway, but the last portion of it might be severely contaminated. Many lighter or smaller airplanes might stop before they even reach the contaminated part at the other

end of the runway and report fair or good braking conditions. The problem then exists for the large and heavy airplanes that might still have substantial speed entering the contaminated part where the braking action becomes "poor" or "nil." That is exactly what happened to the Gemini Air Cargo MD-11F. In reality, runway decontamination should be done completely opposite of how it is currently done: the first portion of the active runway is cleaned from ice and snow, whereas the second half is just barely cleaned. As we have seen in landings (and in rejected/aborted takeoffs), the last two-thirds or the second half of the runway is more critical to stopping, and that is where one wants to have high-friction forces. Landing aircraft would overfly the contaminated part anyway, and the aircraft taking off would use it to accelerate. However, the best choice would be to have the complete runway decontaminated, which is, however, expensive, time consuming, and may cause extensive air-traffic delays.

In Table 3, Schiff [2] summarized the dominant retarding forces according to the runway conditions based on his own investigation and experience in air transportation.

However, we have observed that the reverse thrust delivers about 70%, the aerodynamic drag about 20%, and the brakes only 10% of the retarding force on icy runways. On the dry runway and at high speeds, the friction braking contributes about 60%, reverse thrust 30%, and the aerodynamic braking only 10% of the total retarding force. As the airplane slows down to about 70 kt, the friction braking assumes more than 75% or more of the total stopping effort, whereas the aerodynamic braking becomes negligible.

In our opinion, Schiff's results overestimate aerodynamic braking and are more representative of a fighter jet or a propeller aircraft than a modern civilian jet. In the pilot community, the following landing rules of thumb are often used without any explanation [2,3,14,15]: 1) 100 ft instead of 50 ft over threshold, which adds an additional 900 ft; 2) a 1% increase in airspeed over v_{REF}, which creates a 2% increase in landing ground roll; 3) a 1% weight change, which creates a 1% change in landing ground roll; 4) a 15°F (8.3°C) change from the standard ISA temperature, which creates a 4% change in landing ground roll; 5) a 10 kt wind change, which creates a 15% change in landing ground roll; 6) a 1% uphill runway slope, which creates a 4% decrease in landing ground roll; and 7) a 1% downhill runway slope, which creates a 6% increase in landing ground roll. All these rules of thumb are, in fact, based on the fundamental physical relationships.

Now we will discuss the improvements in our model compared with previous studies. Many authors in previous studies assumed the threshold crossing speed to be 30% above the stalling speed, whereas the touchdown speed was set to be 15 or even 10% above the stalling speed in the landing configuration. For example, a stalling speed of 110 kt in the landing configuration would translate into a minimum of 16.5 kt of airspeed bleed off during the 5–6 s until touchdown. Accordingly, such a descending air-run deceleration of 3 kt/s is clearly hard to explain. It is more likely that the slick jet plane will loose only 5–6 kt in that same time period, which it does, unless it floats for a prolonged period. Also, every author mentioned so far assumed a tangential, zero sink, touchdown. Almost none of the previous studies considered the hydroplaning phenomenon and the speed-dependent rolling friction. Many of these previous models are not comprehensive or complete enough to be used as reliable landing calculators. Many of them do not have any flexibility and do not allow for any variations in piloting performance and technique. Most of these models assume that, once the aircraft has touched down with the main wheels, a maximum braking effort is immediately commenced. In real airplanes, delays exist in the ground lift-dump system deployment, antiskid braking, reversers unlocking, and negative thrust production. Also, the pilot may be too slow in lowering the nose gear.

Table 3 Relative contribution of stopping forces according to Schiff [2]

	Brakes, %	Reverse thrust, %	Aerodynamic drag, %
Dry runway	55	15	30
Wet runway	30	30	40
Icy runway	20	30	50

The strength and the novelty of the approach presented here is that it is comprehensive and treats all the phases of the landing run in sufficient detail. The flare model presented here describes aircraft landing behavior more realistically. Different kinds of runway contamination and hydroplaning phenomena are included and the rolling friction is surface and ground speed dependent. Variations in piloting techniques are fully accounted for. The wind intensity and direction are also incorporated in the model.

VI. Conclusions

An efficient mathematical model capable of handling large-transport-category airplane landing operations was developed. The simulation program was written in MATLAB® and includes an in-house-developed fast, accurate, and simple ODE solver. Convergence, number of iterations, and error control are part of the solver. A new model of flare maneuver has been introduced that removes the unrealistic aircraft behavior used in previous studies. Our model is powerful, yet fast enough, to be used as an operational landing distance calculator and as an educational demonstrator. Our model does not make unrealistic predictions about touchdown speeds; rather, it allows for floating, bouncing, and ballooning and incorporates realistic aircraft behavior.

Pilot performance and techniques, some of which are accepted in the aviation industry and comply with the FAA/Joint Aviation Authorities/ICAO rules, have been taken into account. This feature could provide a tool for the investigation of aircraft landing accidents as well as help in the development of SOPs. We were able to test and calibrate the simulation model against the existing analytical solutions and some certification landing data. The strength of the program is its speed and flexibility in simulating various kinds of operational situations and time-delayed functions with the inclusion of airport, atmospheric, and weather data. Simulation results showed that a 115% FAA-mandated wet-runway correction to an already built-in safety factor of 167% over the actual landing distance may not be adequate for all situations. An airplane might not be able to stop on the usable runway when a particular combination of adverse effects and runway contaminations exist, even though no specific FAA or SOP rule is violated.

However, there is still much space for improvements. The model is not very accurate for speeds below 3–4 kt. The model does not simulate the rolling- and/or sliding-friction coefficient variation along the runway. We need even more realistic aerodynamic data for OGE and IGE parameters that can be verified independently. The coupled nonlinear ODE of flare transition, float, and nose gear derotation roll will be fully simulated in the future. We also plan to obtain manufacturer's data on the particular turbofan engine characteristics to have more accurate reverse-thrust data, which is critical factor on slick runways. The future improved model will partition any runway into 100 ft sections with the intrinsic friction coefficients, liquid, slush and snow thicknesses, and other relevant parameters. In this way, we will be able to more realistically simulate landing operations when some parts of the runway are in good condition and other parts are contaminated. Often, the runways are heavily contaminated with the rubber deposit from tires at locations between 500 and 2500 ft from the threshold. With moderate rain, those parts can become as slick as ice, which might be a big problem in landing ground rolls and rejected takeoffs conducted from the opposite side of the runway.

Acknowledgment

The authors would like to thank Rajeev Shakya, an automotive engineering student from Minnesota State University, for help in designing some illustrations.

References

[1] Blake, W., and Elliott, R. L., "The Last Two Minutes," *Boeing Airliner*, Jan.–March 1991, pp. 1–9.

[2] Schiff, B., *The Proficient Pilot*, Vol. 3, Aviation Supplies & Academics, Inc., Newcastle, WA, 1997.
[3] Lowery, J., *Professional Pilot*, 2nd ed., Iowa State Univ. Press, Ames, IA, 2001.
[4] Gugeler, M., "Contaminated Runways: A Crash Course in Controlling Airspeed," *Aviation Safety*, Vol. 27, No. 11, Nov. 2007, pp. 16–20.
[5] Bibel, G., *Beyond the Black Box: The Forensics of Airplane Crashes*, Johns Hopkins University Press, Baltimore, MD, 2008.
[6] Job, M., "Let's Go Around," *Air Disaster*, Vol. 1, Aerospace Publications, Weston Creek, Australia, 1994, Chap. 17.
[7] Marchi, R., "Winter Operations on Contaminated Runways," *Airport Technology International*, 1997, pp. 61–63, .
[8] Stephens, W. A., "A Look at the Safety Record and Problem Aspects of Operation on Contaminated Runways," AIAA Paper 74-955, Aug. 1974.
[9] McKinney, D., "Flight Safety Foundation Approach-and-Landing Accident Reduction Task Force Operations and Training Working Group Final Report," Society of Automotive Engineers Paper 1999-01-5585, Oct. 1999.
[10] Anon., "Landing Approach and Flare: Approach Speed Control," *Boeing Airliner*, Dec. 1965, pp. 3–5.
[11] Anon., "Landing Approach and Flare: Stopping Under Adverse Conditions," *Boeing Airliner*, Dec. 1965, pp. 7–12.
[12] Davis, D. P., *Handling the Big Jets*, 3rd ed., Civil Aviation Authority, London, 1971.
[13] Swatton, P. J., *Aircraft Performance Theory for Pilots*, Blackwell Science, Oxford, 2000.
[14] Denton, J., *Airline Pilot: A Guide to Good Practices and Techniques*, DFT Publishing, Auckland, New Zealand, 1993.
[15] Webb, J., and Walker, B., *Fly the Wing*, 3rd ed., Blackwell Publishing, Ames, IA, 2004.
[16] White, M. D., "Proposed Analytical Model for the Final Stages of Landing a Transport Airplane," NASA Ames Research Center TN D-4438, 1968.
[17] Pinsker, W. J. G., "The Landing Flare of Large Transport Aircraft," U.K. Ministry of Technology, Aeronautical Research Council Rept. 3602, Nov. 1967.
[18] Seckel, E., "The Landing Flare: An Analysis and Flight-Test Investigation," Princeton University for NASA Langley Research Center CR-2517 1975.
[19] Asselin, M., *An Introduction to Aircraft Performance*, AIAA Education Series, AIAA, Reston, Virginia, 1997.
[20] Mair, W. A., and Birdsall, D. L., *Aircraft Performance*, Cambridge Univ. Press, Cambridge, England, U.K., 1992.
[21] Vinh, N. X., *Flight Mechanics of High-Performance Aircraft*, Cambridge Univ. Press, Cambridge, England, U.K., 1993.
[22] Roskam, J., and Lan, C. T., *Airplane Aerodynamics and Performance*, DARcorporation, Lawrence, KS, 1997.
[23] Phillips, W. F., *Mechanics of Flight*, Wiley, Hoboken, NJ, 2004.
[24] Croll, J. B., and Martin, J. C. T., "Determination of Aircraft Landing Distance on Winter Contaminated Runway Surfaces as a Function of the Canadian Runway Friction Index (CRFI)," *Canadian Aeronautics and Space Journal*, Vol. 45, No. 4, 1999, pp. 358–368.
[25] Yager, T. J., "NASA Boeing 737 Aircraft Test Results from 1996 Joint Winter Runway Friction Measurement Program," NASA Langley Research Center NASA-TM-110482, 1996.
[26] Visser, H. G., "Optimization of High Angle-of-Attack Approach to Landing Trajectories," *Proceedings of the Institution Of Mechanical Engineers. Part G, Journal of Aerospace Engineering*, Vol. 219, No. 6, 2005, pp. 497–506. doi:10.1243/095441005X33394
[27] National Transportation Safety Board Rept. DCA99MA060, File No. 11847 LITTLE ROCK, AR Aircraft Reg. No. N215AA, Time (Local): 23:51 CDT, 01 June 1999
[28] NTSB Report NYC03IA117, File No. 17615 Jamaica, NY Aircraft Reg. No. N703GC, Time (Local): 04:31 EDT, 30 May 2003
[29] Transport Safety Board of Canada Aviation Investigation Rept. A00Q0094, Runway Excursion, Royal Air Maroc, Boeing 747-200 CN-RME, Dorval, Quebec, 23 July 2000.
[30] Fiorino, F., "Making Landings Safer," *Aviation Week and Space Technology*, Vol. 164, No. 26, June 2006, p. 46.
[31] Johnsen, O., "Improving Braking Action," *AeroSafety World*, Aug. 2007, pp. 36–40.
[32] National Transportation Safety Board Preliminary Rept. DCA06MA009, Chicago Midway, Southwest B 737-700, N471WN, 08 Dec. 2005.
[33] Horne, W. B., "Skidding Accidents on Runways and Highways Can Be Reduced," *Astronautics and Aeronautics*, Vol. 5, Aug. 1967, pp. 48–55.
[34] Norrbom, B., and Fristedt, K., "Studies Concerning Snow, Ice and Slush on Runways," The Aeronautical Research Institute of Sweden Memorandum 106, MU-792/862/934, 1975.
[35] Yager, T. J., and McCarty, J. L., "Friction Characteristics of Three 30x11.5-14.5, Type VIII, Aircraft Tires with Various Tread Groove Patterns and Rubber Compounds," NASA Langley Research Center NASA-TP-1080, 1977.
[36] Calkins, D. E., "Aircraft Accident Flight Path Simulation and Animation," *Journal of Aircraft*, Vol. 31, No. 2, 1994, pp. 376–386. doi:10.2514/3.46497
[37] Ferziger, J. H., *Numerical Methods for Engineering Applications*, Wiley, New York, 1981.
[38] Kimberlin, R. D., *Flight Testing of Fixed-Wing Aircraft*, AIAA Education Series, AIAA, Reston, VA, 2003, p. 459.